Int. J. Heat Mass Transfer. Vol. 19, pp. 1135–1142. Pergamon Press 1976. Printed in Great Britain

PEAK BOILING HEAT FLUX ON CYLINDERS IN A CROSS FLOW

JOHN H. LIENHARD* and ROGER EICHHORN
Professors of Mechanical Engineering, University of Kentucky, Lexington, KY 40506, U.S.A.

(*Received* 2 *March* 1976)

Abstract—Analyses of the peak boiling heat flux have traditionally treated either pool boiling or flow boiling situations. Little has been done toward showing how the two processes relate to one another, though observations of burnout on cylindrical heaters have bridged the two situations. This study analyses burnout of horizontal cylinders in a vertical crossflow of increasing velocity, and it reports additional observations in water, methanol and isopropanol.

At very low flow rates the structure of escaping jets changes from three to two dimensional. A criterion for the Helmholtz instability of the two-dimensional jets (or vapor sheets) is obtained from a simple mechanical energy balance. The result is a burnout prediction which is accurate at low to moderate velocities. At high velocities the wake appears to narrow and the prediction must be used as a correlation involving a constant which characterizes the sheet width. In both regimes the equations are generally accurate within $\pm 20\%$. Criteria are also given for the two transitions described above.

NOMENCLATURE

- A, area; subscript j denotes vapor-jet cross-section, and h denotes heater;
- g, gravitational acceleration;
- h_{fg}, latent heat of vaporization;
- q_{max}, peak (or "burnout") heat flux;
- q_{max_p}, peak pool boiling heat flux;
- q_{max_Z}, Zuber's peak heat flux on an infinite horizontal plate, equation (2);
- R, radius of heater;
- R', dimensionless heater radius, equation (2);
- U_g, velocity of escaping vapor in a jet relative to the approaching liquid;
- U_H, Helmholtz unstable value of U_g;
- U_∞, velocity of vertical liquid flow imposed on heater;
- We_g, Weber number based on vapor density, $2R\rho_g U_\infty^2/\sigma$;
- α, ratio of width of two-dimensional vapor jet to diameter of cylinder;
- δ, thickness of vapor blanket on heater at the diametral plane;
- λ_d, dominant Taylor unstable wavelength;
- λ_H, Helmholtz unstable wavelength;
- ρ_f, ρ_g, saturated liquid and vapor densities;
- σ, surface tension between a saturated liquid and its vapor;
- mhv, subscript denoting the maximum value of $\pi q_{max}/\rho_g h_{fg} U_\infty$ obtained from the high-velocity model.

INTRODUCTION

IN THE first quarter century after Nukiyama [1] described the peak heat flux phenomenon in pool boiling, it gradually became apparent that "burnout" could be quite a different matter in flow boiling situations. The Zuber [2]–Kutateladze (see e.g. [3]) theory for the peak pool boiling heat flux, q_{max}, on horizontal flat plates evolved late in this period. While the Zuber–Kutateladze expression has occasionally been applied to wrong configurations, most people who observed that *flow* boiling could improve pool boiling heat fluxes by one or two orders of magnitude weren't even tempted to use that equation to describe it. Instead they tried to develop new descriptions of burnout as they saw it occurring under flow conditions.

From the late 1950's until the present, two entirely different lines of peak heat flux research have developed. The flow boiling efforts (see e.g. [4]) and the hydrodynamic theory of pool boiling (see e.g. [5]) have progressed independently. While this is the way things must be in many cases, we believe that much might be learned by progressing from pool to flow boiling in creating a flow boiling burnout description. To our knowledge this has so far been done only by Andrews and Mohan Rao [6]. They considered ribbons under a vertical downflow and suggested qualitative adaptations of Zuber's formula† to get correlations of q_{max} under flow conditions.

This paper will try to make the connection for a somewhat simpler process, namely a horizontal cylinder in a vertical upward flow of saturated liquid. Beecher as well as Vliet and Leppert (see discussion in [7]), and Cochran and Andracchio [8] have provided measurements of q_{max} for water in this configuration, and [8] has added data for Freon 113. Although Vliet and Leppert developed a semi-empirical theory and correlated their water data with it Cochran and Andriacchio noted that their expression was not applicable to Freon 113.

*Visiting Professor, Chemical Engineering Dept., University of Exeter, Exeter, England, during much of the present study, under partial support of the Science Research Council.

†Actually Zuber's formula does not apply to finite horizontal ribbons, but since they used it qualitatively, that is not a serious objection.

A horizontal cylinder in a vertical crossflow is a good configuration to begin with for two reasons. The single cylinder is the building block of a tube bundle and a solution might provide a base for attacking that far more complex problem. Furthermore the corresponding pool boiling limit has been analysed by Sun [9] and the peak heat flux mechanism is well understood in a stationary liquid.

The aim of this work is to analyse the peak pool boiling heat flux after Sun's mechanism is distorted by the imposition of increasing crossflow. To verify this analysis we will present Min's [10] q_{max} data for methanol (as well as water) flowing over horizontal wires. And we shall present some new observations made in isopropanol.

PEAK HEAT FLUX AT LOW VELOCITY

Sun's expression for the peak pool boiling heat flux, q_{max} (as changed slightly by Lienhard and Dhir [5, 11] to fit a more general statement of the hydrodynamic theory) is:

$$\frac{q_{max_p}}{q_{max_Z}} = \begin{cases} 0.94/(R')^{1/4}, & \text{for } 0.12 < R' \leqslant 1.17 \\ 0.904, & \text{for } R' \geqslant 1.17 \end{cases} \quad (1)$$

where q_{max_Z} is Zuber's expression for q_{max_p} on an infinite horizontal flat plate and R' is the dimensionless heater radius (or square root of the Bond number):

$$q_{max_Z} = \frac{\pi}{24}\rho_g^{1/2} h_{fg} \sqrt[4]{[\sigma g(\rho_f - \rho_g)]};$$

$$R' = \frac{R}{\sqrt{\left[\dfrac{\sigma}{g(\rho_f - \rho_g)}\right]}}. \quad (2)$$

Equations (1) are based on the assumed vapor escape configurations shown in Fig. 1. They presume that the peak heat flux is reached when the jets become Helmholtz unstable owing to the collapse of an axial disturbance of wavelength, λ_H, in the jet walls. The collapse occurs when the vapor velocity relative to the liquid, U_g, in the jets reaches the value, U_H, sufficient to trigger Helmholtz instability. This value is known [12] to be:

$$U_H = \sqrt{\left[\frac{2\pi\sigma}{\rho_g \lambda_H}\right]}. \quad (3)$$

In the R' range $\leqslant 1.17$, Sun and Lienhard [9] assumed that the jets were spaced on the "most-dangerous" Taylor unstable wavelength,

$$\lambda_d = 2\pi\sqrt{3}\sqrt{\left[\frac{\sigma}{g(\rho_f - \rho_g)}\right]} \quad (4)$$

and that the Helmholtz wavelength was equal to the circumference of the jets, $2\pi(R+\delta)$. These assumptions, and empirical observations of δ, permitted the determination of q_{max_p}.

As a liquid cross-flow is imposed upon this configuration a radical change occurs. The three dimensional jet-like vapor plumes are replaced with a two dimensional vapor sheet as sketched in Fig. 2. The transition should occur when the gravity, inertial, and buoyant forces (characterized by R' and the liquid Weber number, $2R\rho_f U_\infty^2/\sigma$) are in a particular balance. Practically speaking, this occurs at a very low liquid velocity, as we shall discuss subsequently. Accepting this for the moment, we turn first to the behavior of the resulting sheet.

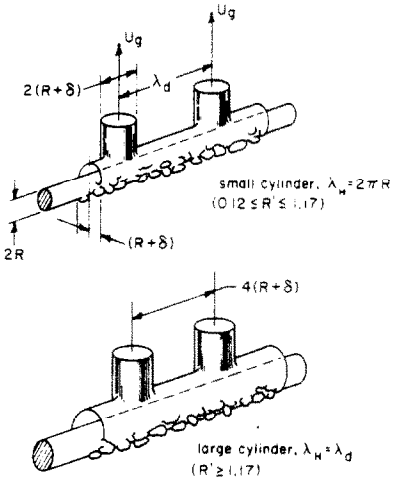

FIG. 1. Sun's model for the liquid–vapor interface during pool boiling from cylinders.

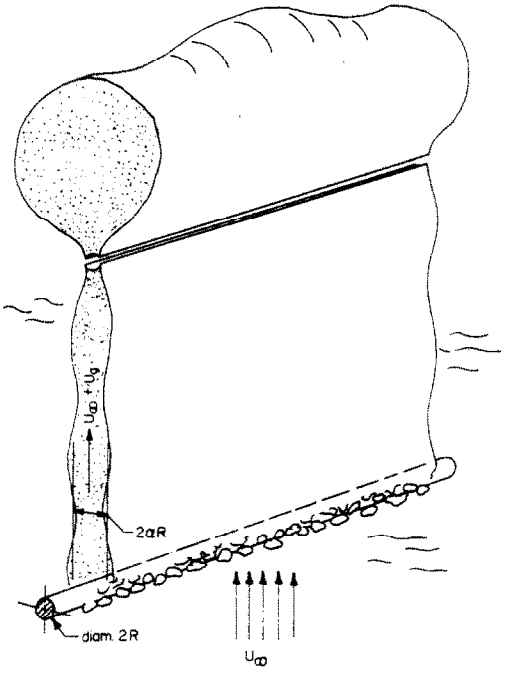

FIG. 2. Vapor removal by the action of two-dimensional jets before burnout occurs.

TWO-DIMENSIONAL JET BURNOUT

The idealization of the vapor removal process shown in Fig. 2 was adapted from experimental observations*

*This picture has been heavily influenced by close study of the experiment [10] under strobe-light illumination.

[7, 8, 10]. The sheets seem to exhibit a faint but regular waviness below a breakoff point. After breakoff, the vapor comes to virtual stagnation relative to the flowing liquid, and the sheet balloons into large sausage-like bubbles which tear loose in very straight lines. While the causal mechanism for this behavior is not known, it clearly starts at heat fluxes far below q_{max} and does not result in burnout. Burnout will occur when the configuration shown becomes unstable. We shall defer the question of specifying the vapor velocity for which this occurs.

The heat flux can be accounted for by the removal of vapor. In this case q_{max} can be written

$$q_{max} = \rho_g h_{fg} U_\infty \frac{A_j}{A_h}\left(1+\frac{U_g}{U_\infty}\right) \tag{5}$$

where U_g is the velocity of the vapor relative to the liquid approach velocity, U_∞. The jet area is A_j and A_h is the heater area. Taking α as the ratio of the actual jet width to the heater diameter gives $A_j/A_h = \alpha/\pi$, and

$$\frac{\pi q_{max}}{\rho_g h_{fg} U_\infty} = \alpha + \alpha\frac{U_g}{U_\infty}. \tag{6}$$

In the pool boiling case, q_{max_Z}, which involves gravity, is used to nondimensionalize q_{max}. Since gravity isn't likely to be important here [unless the liquid inertia is small in comparison with buoyancy and surface tension—a point discussed later in the context of equation (14)], the nondimensionalization given in equation (6) is more appropriate.

The problem of determining q_{max} is now cast in terms of estimating the jet width and the critical jet velocity, U_g. We turn next to these issues.

STABILITY CONSIDERATIONS

The Helmholtz collapse of a thin ($2\alpha R \ll \lambda_H$) vapor sheet is a special case of a general solution given by Hagerty and Shea [13]. The most rapid collapse of such a sheet will occur when the relative velocity, U_g, reaches [cf. equation (3)] a value, U_H, given by

$$\frac{U_H}{U_\infty} = \frac{2\pi}{U_\infty}\sqrt{\left[\frac{3\sigma R}{\rho_g \lambda_H^2}\right]} = 2\pi\left(\frac{3}{2}\right)^{1/2}\frac{1}{We_g^{1/2}}\frac{2R}{\lambda_H} \tag{7}$$

where the Weber number, $We_g = 2R\rho_g U_\infty^2/\sigma$ is based on the vapor density. Equation (7) is awkward because $2R/\lambda_H$ is unknown and we don't see how to guess its value.

This dilemma can be resolved by a simple mechanical energy balance consideration which should be satisfied at burnout: A little above the cylinder the liquid is again moving at U_∞. Hence Fig. 3 shows a control volume which moves upward with velocity, U_∞, relative to the cylinder. The top of the vapor sheet, which is observed to maintain a fixed average distance above the cylinder, will move downward in the control volume at an average speed U_∞. The detached bubbles have negligible surface area per unit volume in comparison with the sheet. Therefore the control volume loses

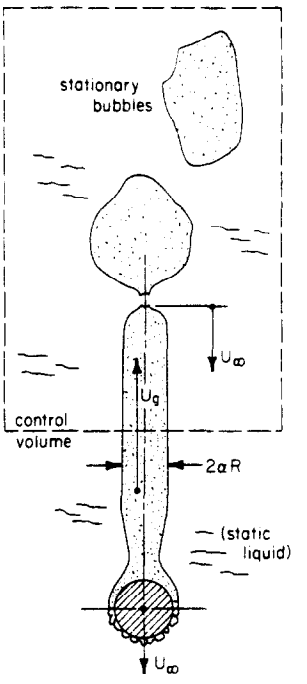

FIG. 3. Control volume for kinetic/surface energy balance.

surface energy at a rate close to $2U_\infty\sigma$ while kinetic energy enters it at a rate equal to* $\rho_g U_g(2\alpha R)U_g^2/2$.

Accordingly the mechanical energy balance on the sheet yields:

$$-2U_\infty\sigma + \rho_g 2\alpha R U_g^3/2 = 0 \tag{8}$$

or

$$\frac{U_g}{U_\infty} = \frac{4^{1/3}}{(\alpha We_g)^{1/3}}. \tag{9}$$

We shall now offer an heuristic argument to the effect that equation (9) defines the value of U_g for which burnout occurs. The argument is speculative, but only in certain features. Burnout will certainly be determined by the relative magnitude of the only two mechanical energy exchanges associated with the sheet. Therefore, even if one questions some of the following suppositions, equation (9) will still determine the burnout vapor velocity within a multiplicative constant.

If U_g is insufficient to satisfy this balance, the phenomenon shown in Fig. 2 will persist. The deficit in incoming energy will be made up by the surrounding liquid which will pull upon the vapor "knob" at the top of the sheet, and stabilize the system. But if U_g exceeds $4^{1/3}U_\infty/We_g^{1/3}$ there *is no* mechanism by which the sheet can transmit the excess energy to the surrounding liquid. A simple calculation shows that viscosity is very ineffective in doing so for the fluids and in the size ranges of interest. Accordingly the vapor must increase in pressure, allowing a conventional Helmholtz collapse to occur.

*A small lateral liquid kinetic energy transfer from the control volume is easily shown to vanish as the control volume width is increased.

The resulting burnout formula is then obtained by substituting equation (9) in (6):

$$\frac{\pi q_{max}}{\rho_g h_{fg} U_\infty} = \alpha + \frac{4^{1/3}\chi^{2/3}}{We_g^{1/3}}. \quad (10)$$

The thickness correction factor, α, will be a number on the order of unity. Attention will next be given to its evaluation.

THE ESTIMATION OF VAPOR SHEET THICKNESS

The presence of an evolving vapor blanket around the cylinder suggests a simplification of the analysis of the flow in its vicinity. The vapor largely removes the no-slip condition between the liquid and the cylinder. Accordingly the liquid flow can be treated as a potential flow. Thus the interface will reach a velocity near $2U_\infty$ at the horizontal diametral plane and then close inward as shown in Fig. 4. This wake behavior will have the additional advantage of suppressing vapor separation behind the cylinder, so the Bernoulli equation can be used to describe both the liquid and vapor flow from station (1) to (2).

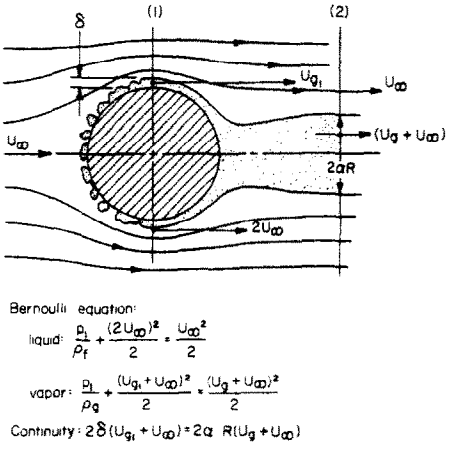

FIG. 4. Potential flow model for the evaluation of α.

The two Bernoulli equations and the continuity equation are shown in the figure. Combining them to solve for α and using equation (9) to eliminate U_g/U_∞ at burnout gives:

$$1 + \frac{4^{1/3}}{(\alpha We_g)^{1/3}} = \frac{\sqrt{[3\rho_f/\rho_g]}}{\sqrt{\left[\alpha^2\left(\frac{R}{\delta}\right)^2 - 1\right]}}. \quad (11)$$

It seems unlikely that α is determined by surface tension. Therefore it should depend on the dimensionless group ρ_f/ρ_g. The vapor blanket thickness, δ, however, should be strongly related to σ and U_∞. We therefore presume that the We_g dependence of the R.H.S. is all vested in (R/δ) and that α can be expressed as a simple power law variation of ρ_f/ρ_g. Since the terms 1 and -1 in equation (11) are negligible in the range of interest we get:

$$\alpha = \text{constant}\,(\rho_f/\rho_g)^{3/4}. \quad (12)$$

Equation (11) is only valid as long as liquid momentum, $\rho_f U_\infty^2$, significantly exceeds the vapor momentum $\rho_g U_g^2$. If this condition is not met the vapor should just flow straight up, without allowing the liquid to curve around the back as predicted by potential flow. In this case α is probably close to unity in all cases, so

$$\frac{\pi q_{max}}{\rho_g h_{fg} U_\infty} = 1 + \left(\frac{4}{We_g}\right)^{1/3}; \text{ for low } U_\infty. \quad (10a)$$

In accordance with the preceding argument we shall look for a transition at a particular value of dimensionless peak heat flux given by

$$\frac{\pi q_{max}}{\rho_g h_{fg} U_\infty} = 1 + \frac{U_g}{U_\infty} = 1 + \text{constant}\sqrt{(\rho_f/\rho_g)} \quad (13)$$

where the constant must be determined on the basis of experimental results.

COMPARISON OF ANALYSIS AND EXISTING DATA

The experiment used to obtain Min's water and methanol data, as well as our own isopropanol data is described in the Appendix. These results and those from [7, 8] are plotted in Fig. 5. These include the unpublished data of Beecher [14]. Actually, only the data for Vliet's two lowest velocities have been included since the remaining velocities show q_{max} decreasing with increasing subcooling near the saturation temperature.

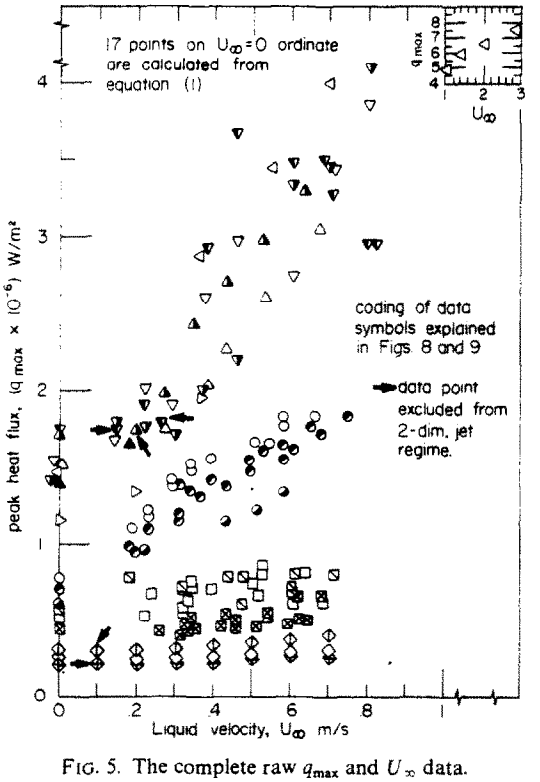

FIG. 5. The complete raw q_{max} and U_∞ data.

The excluded data are high in comparison with those of other authors under comparable conditions, and they could reflect idiosyncracies in Vliet's flow system at higher velocities.

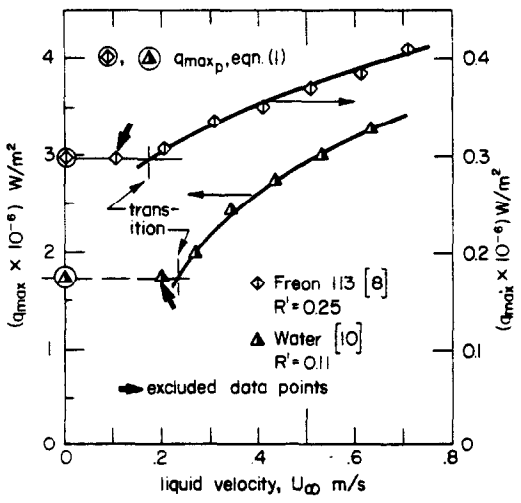

FIG. 6. Typical curves illustrating three-dimensional to two-dimensional jet transition.

Figure 5 can be resolved into a set of figures typified by Fig. 6 which show that the two-dimensional sheet data fall on a line which passes through q_{max_p} at a finite velocity, U_∞. A total of five data marked with arrows on Fig. 5 (and 6) were found to lie on q_{max_p}. These were presumed to represent the three-dimensional jet burnout mode, and were excluded from the subsequent correlations.

The three-dimensional to two-dimensional jet transition point obtained in this way was correlated empirically and found to be given by

$$(We_g)_{\text{transition}} \simeq 4(\rho_f/\rho_g)R'. \tag{14}$$

Equations (10) and (12) suggest that the remaining data should correlate on $\pi q_{max}/\rho_g h_{fg} U_\infty$ vs $(\rho_f/\rho_g)^{1/2}/We_g^{1/3}$ coordinates. This graph is shown in Fig. 7 and the data come together remarkably well in the lower left hand portion of the diagram. Since the water data begin to scatter markedly for $\pi q_{max}/\rho_g h_{fg} U_\infty > 11.5$, we use this point to fix the constant in equation (13) as 0.275. Then with the aid of equation (13) we can complete the list of maximum "high-velocity" values of $\pi q_{max}/\rho_g h_{fg} U_\infty$.

Table 1

Liquid	$\sqrt{(\rho_f/\rho_g)}$	$(\pi q_{max}/\rho_f h_{fg} U_\infty)_{max} = 1 + 0.275\sqrt{(\rho_f/\rho_g)}$
Water	38.2	11.5
Methanol	26.2	8.2
Isopropanol	17.4	5.8
Freon 113	13.0	4.6

All data above the appropriate value of $1+0.275\sqrt{(\rho_f/\rho_g)}$ (or clearly to the right of the correlation region in Fig. 7) have accordingly been plotted in Fig. 8 on the coordinates suggested by the low-velocity model, equation (10a). Equation (10a) has also been plotted on the graph and it lies squarely among the data. The great majority of the measured values of $\pi q_{max}/\rho_g h_{fg} U_\infty$ lie within $\pm 10\%$ of the theoretical values, and 95% lie within $\pm 20\%$.

The remaining data are presumed to lie in the "high-velocity" range and to be described by equations (10) and (12). The slope of the correlation in $\pi q_{max}/\rho_g h_{fg} U_\infty$ vs $\sqrt{(\rho_f/\rho_g/We_g^{1/3}}$ coordinates should be the constant in equation (12) raised to the 2/3 power and divided by $4^{1/3}$. The data in Fig. 7 thus give

$$\alpha = (\rho_f/\rho_g)^{3/4}/169 = \begin{cases} 1.39 \text{ for water} \\ 0.79 \text{ for methanol} \\ 0.43 \text{ for isopropanol} \\ 0.28 \text{ for Freon 113.} \end{cases} \tag{12a}$$

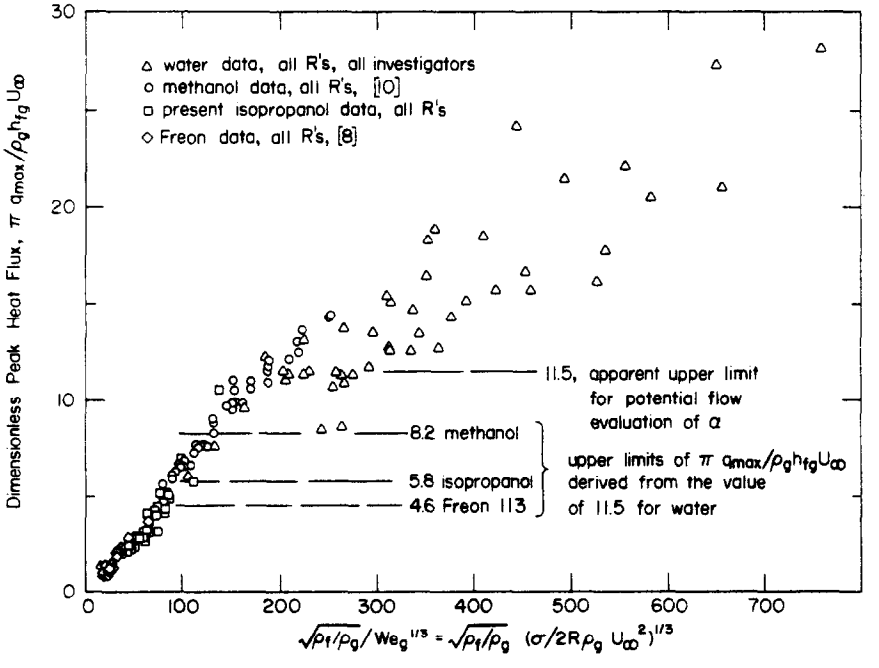

FIG. 7. Dimensionless peak heat flux plotted in accordance with high-velocity model, equations (10) and (12).

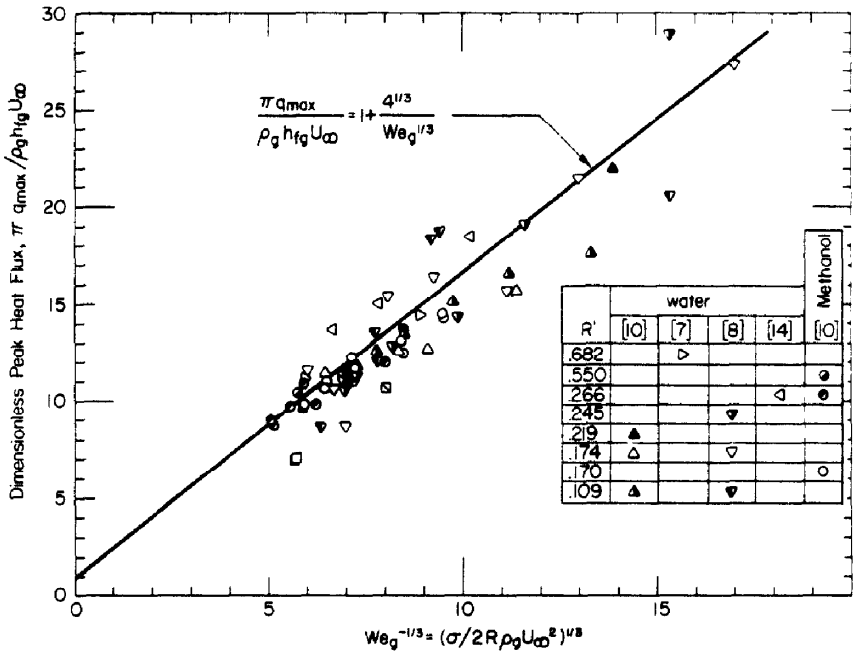

FIG. 8. Comparison of the "low-velocity" prediction of q_{max} with data.

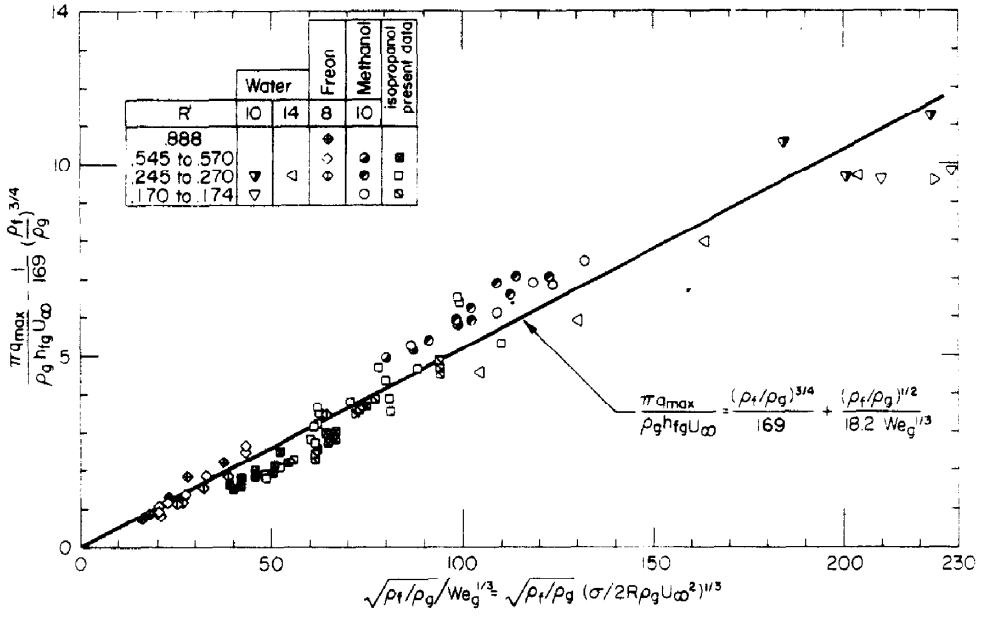

FIG. 9. Comparison of the "high-velocity" prediction of q_{max} with data.

These data are replotted in Fig. 9, in accordance with the final form of equations (10) and (12)

$$\frac{\pi q_{max}}{\rho_g h_{fg} U_\infty} - \frac{1}{169}\left(\frac{\rho_f}{\rho_g}\right)^{3/4} = \frac{1}{19.2}\left(\frac{\rho_f}{\rho_g}\right)^{1/2}\frac{1}{We_g^{1/3}} \quad (15)$$

which represents 85% of the data with $\pm 20\%$ accuracy.

There appears to be a minor systematic error involved in the data scatter here. The water and isopropanol data lie a bit lower than the Freon and methanol data. The reason probably is that α actually exhibits some minor dependence on factors other than the density ratio, contrary to equation (12). However, such small corrections do not appear to be worth pursuing further.

The present equations show that for flow boiling $q_{max} \sim U_\infty^{1/3}/R^{1/3}$. This result retains the essential features of Vliet's correlation for water which showed $q_{max} \sim U_\infty^{1/2}/R^{0.15}$. Of course, without having data for more than one fluid state, Vliet could neither tell what role the relevant thermal properties played, nor guess the significant effect of the ratio ρ_f/ρ_g.

CONCLUSIONS AND RECOMMENDATIONS

(1) As the liquid velocity is increased during boiling from a horizontal cylinder in a vertical crossflow Sun's pool boiling model applies only up to the point described by equation (14).

(2) A first transition then occurs in which a two

dimensional vapor sheet replaces the three dimensional Sun–Zuber jets. Burnout can be predicted within $\pm 20\%$ accuracy in the low-velocity, two-dimensional sheet regime, by equation (10a).

(3) A second transition occurs at increased liquid velocity. The flow in the sheet and its terminal velocity can now be described by a simple potential flow model. This transition occurs when

$$\pi q_{max}/\rho_g h_{fg} U_\infty = 0.275(\rho_f/\rho_g)^{1/2} + 1.$$

(4) The flow in the high-velocity regime is described within $\pm 20\%$ accuracy by the one-constant correlation given in equation (15).

(5) In the flow mechanisms presented here, gravity is taken to be unimportant. Yet no one has produced experimental data in a downflow. The data studied here probably are gravity-independent since no rods larger than 0.32 cm in diameter are represented. But larger heaters, or a different flow direction might well reveal gravity influences not evident here.

(6) The mechanism which shapes the break-off of the sheets should be explained. (It might be dictated in part by the influences of gravity.)

(7) The sheet thickness and the factors that determine it should be studied further.

Acknowledgement—We are grateful to Mr. Thomas K. Min who not only provided the measurements quoted in [10] but also assisted in the measurements of q_{max} in isopropanol. The construction of the apparatus was one of the last major undertakings of Mr. E. R. Hoover before his untimely death in December of 1974. We are grateful for this and his many other contributions.

REFERENCES

1. S. Nukiyama, The maximum and minimum values of the heat Q. Transmitted from metal to boiling water under atmospheric pressure, *Trans. Japan. Soc. Mech. Engrs* **37**, 367 (1934).
2. N. Zuber, Hydrodynamic aspects of boiling heat transfer, AEC Report AECU-4439, Physics and Mathematics (June 1959).
3. S. S. Kutateladze, *Fundamentals of Heat Transfer*, edited by R. D. Cess, Chapter 18. Edward Arnold, London (1963).
4. J. G. Collier, *Convective Boiling and Condensation*. McGraw-Hill, London (1972).
5. J. H. Lienhard and V. K. Dhir, The extended hydrodynamic theory of the peak and minimum pool boiling heat fluxes, NASA CR-2270 (1973).
6. D. G. Andrews and P. K. Mohan Rao, Peak heat fluxes on thin horizontal ribbons in submerged water jets, *Can. J. Chem. Engng* **52**, 323–330 (1974).
7. G. Leppert and C. C. Pitts, Boiling, in *Advances in Heat Transfer*, edited by T. F. Irvine, Jr. and J. P. Hartnett, Vol. 1. Academic Press, New York (1964).
8. T. H. Cochran and C. R. Andracchio, Forced convection peak heat flux on cylindrical heaters and refrigerant 113, NASA D-7553 (February 1974).
9. K. H. Sun and J. H. Lienhard, The peak pool boiling heat flux on horizontal cylinders, *Int. J. Heat Mass Transfer* **13**, 1425–1439 (1970).
10. T. K. Min, Masters thesis, Mech. Engr. Dept., Univ. of Kentucky, Lexington, Ky (1975).
11. J. H. Lienhard and V. K. Dhir, Hydrodynamic prediction of peak pool boiling heat fluxes from finite bodies, *J. Heat Transfer* **C95**(2), 152–158 (May 1973).
12. Sir H. Lamb, *Hydrodynamics*, 6th edn. Dover, New York (1945).
13. W. W. Hagerty and J. F. Shea, A study of the stability of plane fluid sheets, *J. Appl. Mech.* **22**, 509–514 (December 1955).
14. N. Beecher, M. S. Thesis in Chem. Engng, M.I.T. (1948) (cited in [7]).

APPENDIX

New Data for Water, Methanol and Isopropanol

The hitherto unpublished data of Min [10] for water and methanol and our own measurements for isopropanol were obtained in the following experiment.

Apparatus and procedure

The apparatus is described in full detail in [10]. It consists of a variable speed pump, which circulates a liquid through a heater to bring it close to saturation, and then forces it upward through a nozzle onto the test heater.

The nozzle is an 8.9×1.9 cm rectangle supplied by an 8.9 cm square plenum. It is tapered 30° on either side and terminates in a straight run, 1.9 cm in length. The nozzle protrudes 1.9 cm into a 13 cm square box which spills into an open collection tank about 22 cm above the nozzle exit. Local atmospheric pressure at this point is about 0.975 atm. From here the liquid is recirculated.

Peak heat flux measurements were made on horizontal cylindrical heaters fixed about 0.5 cm above the nozzle exit plane. The flow at this station was measured in cold water using a hot film anemometer and found to be uniform within $\pm 6\%$ of the mean velocity. The mean velocity was obtained in the experiments with an orifice meter.

The cylindrical heaters on which q_{max} was observed were electrical resistors made of nichrome wire, or thin-walled stainless steel tubing. The former had diameters of 0.051, 0.081 or 0.102 cm while the latter was 0.165 cm in diameter. The cylinders were suspended from above by two 0.64 cm dia brass electrodes.

In the water tests, swaged 0.3 cm dia copper leads were attached to the nichrome heaters. The portion of these terminals which protruded into the flow was tapered to eliminate end effects. For the methanol and isopropanol tests leads of the same size and shape were electroplated directly to the ends of the heating elements. The wires were heated by A.C. current supplied from two auto-transformers in series (except for a few D.C. data in isopropanol). q_{max} was computed from voltage and current readings at burnout, or from a single voltage reading and a prior measurement of the D.C. resistance when this was feasible.

With water it was not possible to hold the flow loop at the boiling point without having cavitation bubbles rising with the jet. These disturbed both the flow rate measurements as well as the flow field around the heating element. To avoid these problems the flow loop was first brought up to saturation temperature and then measurements taken while it cooled down. With water, each measurement resulted in failure of the wire. It was possible to replace the wires and make a new measurement while the temperature of the loop decreased by only a few degrees. Five or six of such measurements were made at each flow rate, and the results were extrapolated to zero subcooling to find the burn-out point for saturated water. With methanol and isopropanol, this procedure was not necessary, since the flow loop could be operated within about 0.5°C of the saturation temperature.

A total of 12 q_{max} observations in water, 39 in methanol and 55 in isopropanol, were obtained in this manner. The water and methanol results are presented in [10]. The complete raw data, including our own subsequent isopropanol data, are available on request. In this paper, these data are only given graphically. Somewhat fewer than the total of 106 new measurements are displayed since some of them are duplicates.

TRANSFERT DE CHALEUR CRITIQUE PAR EBULLITION AUTOUR DE CYLINDRES EN ATTAQUE TRANSVERSALE

Résumé—Les études de flux de chaleur maximal par ébullition sont généralement relatives soit à l'ébullition d'un liquide au repos soit à l'ébullition dans un écoulement. Peu a été fait afin de montrer comment les deux processus sont liés l'un à l'autre, bien que les observations d'assèchement sur les échangeurs cylindriques aient réunis les deux situations. La présente étude analyse l'assèchement de cylindres horizontaux dans un écoulement vertical de vitesse croissante, et fait état d'observations supplémentaires dans l'eau, le méthanol et l'isopropanol.

Aux très faibles débits la structure tridimensionnelle des jets qui s'échappent devient bidimensionnelle. Un critère pour l'instabilité de Helmholtz dans les jets bidimensionnels (ou les couches de vapeur) est obtenu à partir d'un simple bilan d'énergie mécanique. Cela permet une prévision suffisamment précise de l'assèchement aux vitesses faibles et modérées. Aux vitesses élevées le sillage se rétrécit et la prévision doit être utilisée comme une relation comportant une constante qui caractérise l'épaisseur de la couche. Dans chacun des régimes les équations fournissent généralement une précision de $\pm 20\%$. Des critères sont également donnés pour les deux transitions décrites précédemment.

KRITISCHE HEIZFLÄCHENBELASTUNG BEI QUERANGESTRÖMTEN ZYLINDERN

Zusammenfassung—Analysen des maximalen Wärmestroms haben traditionsgemäß entweder die Situation beim Behältersieden oder beim Sieden in Strömungen behandelt. Die wechselseitige Verbindung beider Prozesse wurde wenig beachtet, obwohl die Beobachtungen des burnout an zylindrischen Heizflächen die beiden Situationen überbrücken. Die vorliegende Untersuchung analysiert den burnout an horizontalen Zylindern bei vertikaler Querströmung zunehmender Geschwindigkeit und liefert weitere Beobachtungen in Wasser, Methanol und Isopropanol.

Bei sehr kleinen Anströmraten ändert sich die Struktur der abströmenden Strahlen von drei- auf zweidimensional. Ein Kriterium für die Helmholtz-Instabilität der zweidimensionalen Strahlen (oder Dampfschleier) erhält man aus einer einfachen mechanischen Energiebilanz. Das Ergebnis ist eine burnout-Gleichung für geringe und mittlere Geschwindigkeiten. Bei hohen Geschwindigkeiten scheint sich die Nachlaufströmung zu verengen und die Gleichung muß eine Konstante enthalten, die charakteristisch für die Schleierbreite ist. In beiden Fällen sind die Gleichungen im allgemeinen innerhalb von $\pm 20\%$ genau. Kriterien für die beiden beschriebenen Fälle sind angegeben.

МАКСИМАЛЬНЫЙ ТЕПЛОВОЙ ПОТОК ПРИ КИПЕНИИ НА ЦИЛИНДРАХ В ПОПЕРЕЧНОМ ПОТОКЕ

Аннотация — Обычно максимальный тепловой поток при кипении рассматривался применительно к процессам кипения в большом объеме или в потоках. Их взаимосвязь почти не отражалась, хотя исследование критического теплового потока на цилиндрических нагревателях позволило связать эти два процесса. Проведен анализ кризиса кипения на горизонтально расположенных цилиндрах при наличии вертикального потока жидкости, скорость которой возрастает. Исследования проводились в воде, метане и изопропаноле. При очень малых скоростях потока трехмерные истекающие струи становятся двумерными. На основе простого механического баланса энергии получен критерий неустойчивости Гельмгольца для двумерных струй (или слоев пара). Рассчитан критический тепловой поток для малых и средних значений скорости. При больших скоростях след сужается, и в расчетную формулу необходимо вводить постоянную для ширины слоя. В обоих случаях уравнения имеют точность $\pm 20\%$. Также приводятся критерии для двух вышеописанных переходов.